

ELECTRONIC OZONE SPECTROSCOPY.

I. STRUCTURE OF LOW-LYING ELECTRONIC STATES

I.M. Sizova

*P.N. Lebedev Physics Institute
of the Russian Academy of Sciences, Moscow
Received February 3, 1993*

Experimental and theoretical studies of electronic structure and electronic absorption spectra of one of the most important minor constituents of the atmosphere, namely, the ozone molecule, are summarized through 1991. The range of the wavelengths from the near infrared (dissociation energy of the ground electronic state of O₃) to the far ultraviolet (the first ionization potentials of O₃) is considered.

The present paper is the first part of a review and includes a general description of electronic absorption spectra, structure of electronic levels, and a more detailed information about the energy region near the dissociation threshold of the ground electronic state.

1. GENERAL DESCRIPTION OF THE ABSORPTION SPECTRUM AND THE STRUCTURE OF ELECTRONIC LEVELS OF O₃

Ozone was discovered in 1840 (see Ref. 1), and in the 1880's–1890's its major absorption bands in the visible and UV spectral regions, namely, the Hartley 200–310 nm band (1881, see Ref. 2), the Chappuis 450–800 nm band (1882, see Ref. 3), the Huggins 310–360 nm bands (1890, see Ref. 4) were found. Starting in the 1930's and until the present time the measurements of the O₃ absorption coefficient over a wide range of wavelengths at different temperatures were repeatedly made. The obtained data (many of them are shown in the figures) correlate well, and the extensive studies by Vigroux, Inn, and Tanaka made back in the 1950's are still significant.

The ozone molecule is a triatomic system with 18 valence electrons of S_{2v} symmetry and AB₂ type with the vertex angle $\theta \approx 117^\circ$ and two equal bonds $R \approx 1.3 \text{ \AA}$ in the ground electronic state.

According to the Hartree–Fock single–configuration model, the lowest electronic state of O₃ should be the triplet state ³B₂, however, the ozone molecule is poorly described by the Hartree–Fock single–particle theory^{5,6} because of the biradical structure of its ground state. This is true for the neutral molecule and its ions. In general, the ozone molecule is characterized by a noticeable contribution of its many configurations to all electronic states.

The ground state of O₃ is the biradical singlet state X¹A₁(4π) and consists of two configurations Φ₁ and Φ₂ to the extent of 90%, namely, $\Psi(X^1A_1) \approx c_1\Phi_1 + c_2\Phi_2 = = 1a_1^2 2a_1^2 1b_2^2 3a_1^2 2b_2^2 4a_1^2 5a_1^2 3b_2^2 4b_2^2 6a_1^2 1b_1^2 (c_1 \cdot 1a_2^2 + c_2 \cdot 2b_1^2)$, where $c_1^2 = 79\%$ and $c_2^2 = 11\%$ (see Refs. 7–10). The former configuration Φ₁ is the Hartree–Fock determinant, and the latter configuration Φ₂ is its doubly excited state.

The biradical structure of X¹A₁ was firstly described by Hay et al.⁷ in 1973–1975. They obtained the basic formula $\Psi(X^1A_1) \approx 0.876 \cdot 1a_2^2 - 0.481 \cdot 2b_1^2$, i.e., 77% of 1a₂²

and 23% of 2b₁². In subsequent computations the contribution of the latter configuration was markedly smaller (79.3% of 1a₂² and 10.7% of 2b₁² according to Ref. 8). The biradical character of the structure X¹A₁ was analyzed in Ref. 9 in great detail. To calculate the contribution of two basic radicals within the framework of multiconfiguration self–consistent field method, 13413 configurations were involved, i.e., all singly and doubly excited states relative to Φ₁ and Φ₂. Laiding and Schafer⁹ obtained $\Psi(X^1A_1) \approx 0.8870 \cdot 1a_2^2 - 0.3371 \cdot 2b_1^2$, i.e., 78.7% of 1a₂² and 11.4% of 2b₁², which corresponds to the contribution of biradical $B = c_2^2 (1/\sqrt{2})^2 = 22.7\%$.

In the context of the generalized valence bond model¹⁰ describing diabatic electron energy surfaces (theory of diabatic surfaces was developed in detail by Smith [Phys. Rev. **179**, No. 1, 111 (1969)]) the surface X¹A₁(4π) crosses the single–configuration state ¹A₁(6π), where $\Psi(^1A_1) \approx \dots 4b_2^2 1b_1^2 1a_2^2 2b_1^2$ (this configuration is formed from the ground determinant Φ₁ due to two–electron transition 6a₁² → 2b₁² or from the second configuration Φ₂ due to two–electron transition 6a₁² → 1a₂²). Within the limits of pseudo–adiabatic approach these two surfaces of the same symmetry repulse from each other interacting in the region of intersection (avoided crossing and/or conical crossing) and form two adiabatic surfaces. A lower adiabatic surface ¹A₁ has two local minima: the first X¹A₁, being of C_{2v} symmetry with $\theta \approx 117^\circ$ (open structure of O₃) and the second of D_{3h} symmetry with $\theta = 60^\circ$ (closed ring structure of O₃). The structure of the upper surface ²A₁ is described below when considering the main UV absorption band of O₃, i.e., the Hartley band. By repulsing in the region of intersection, the diabatic surfaces ¹A₁ form the minimum of the adiabatic surface ²A₁ and, simultaneously, the potential barrier between the open and ring structures of O₃ in the ground state ¹A₁ (see Fig. 1). As a result, two structures of the ground electronic state of O₃ (open and ring) are

separated by the high potential barrier which makes them to be practically independent states. The transition between them is the two-electron transition ($4\pi \rightarrow 6\pi$), as it can be seen from the above formulas. The structure of these surfaces is described in more detail below when considering the ring structure of ozone (Sec. 2) and the

Hartley band. A schematic interpretation of electronic bonds in the ground state of O_3 with its biradical structure in terms of superposition of the states is given, for example, in Ref. 11 and is based on evidence derived from the results of *ab initio* calculations of valence bond as compared to other available methods of calculations.

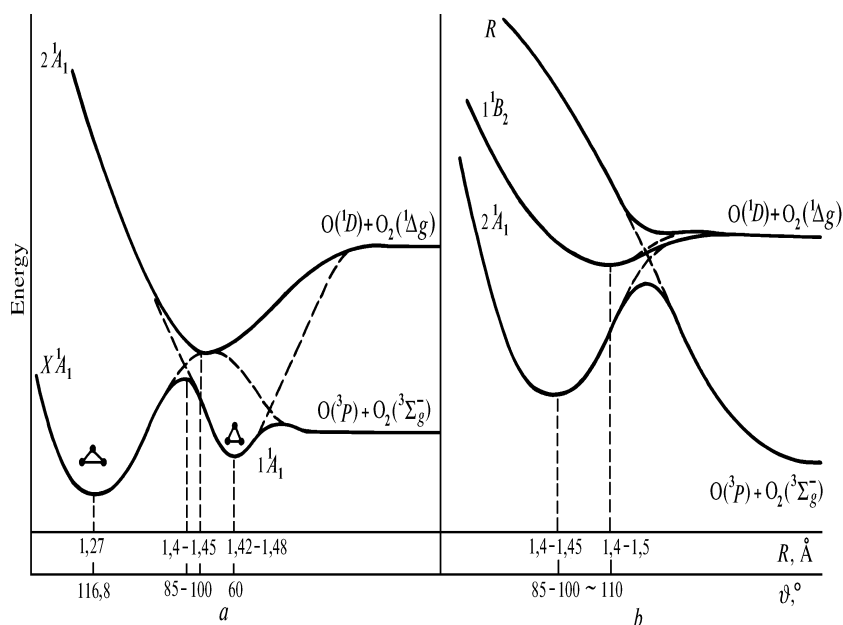


FIG. 1. Schematic illustration of crossing (and repulsion) of the surfaces 1^1A_1 and 2^1A_1 (a) as well as of the surfaces 2^1A_1 and 1^1B_2 and the repulsive surface R in the region between the Huggins bands and the Hartley band (b). The real pattern is four-dimensional.

By now a great number of theoretical calculations of the potential surface of the lower state 1^1A_1 has been made. There are *ab initio* calculations near the equilibrium X^1A_1 (see, for example, Ref. 12 and references therein) together with their approximations by simple fitting models (e.g., Ref. 13) and semiempirical calculations of the entire surface which differ in their complexity and accuracy of fitting the experimental spectroscopic data, critical states of the products of dissociation at large separations, symmetry properties, and results of *ab initio* calculations (see, for example, Ref. 14).

The best known potential surfaces of the ground state of the ozone molecule are the Sheppard–Walker surface¹⁵ derived from *ab initio* calculations of the points in the region of the surface minimum and fitted to the standard shape of the Sorbey–Murrell surface and the Carters–Mills–Murrell–Varandas surface¹⁶ obtained by the Whitehead–Handey procedure. Since both surfaces ignore the experimental data on the upper vibrational levels, they differ sharply in the region of multiple excitation of vibrational quanta of O_3 , as shown in Ref. 17, and both produce the vibrational levels being absolutely inconsistent with the experimental data obtained in this region. To eliminate this disadvantage,

the authors of Ref. 17 proposed a new procedure of empirical parametric fitting of the surface based on the spectrum of the high vibrational levels. The surface found in Ref. 17 and described by 8 parameters retrieved from the spectrum of modes ν_1 and ν_3 with allowance made for up to 6 quanta (21 vibrational levels) yields the spectrum being quantitatively very close to the experimental spectrum of high vibrational levels of these modes (error is $\sim 7.2 \text{ cm}^{-1}$ for an experimental accuracy of $\sim 10 \text{ cm}^{-1}$) and is the best surface of the ozone molecule up to energies $\sim 6500 \text{ cm}^{-1}$, in the authors' opinion. Further advantage can be gained on this way if bending oscillation, rotation, and possible potential barrier to dissociation of molecules are accounted for.

The spectrum of O_3 is in many respects analogous to the spectra of similar molecules, for example, SO_2 (see Refs. 18–20). Practically the entire expanded absorption spectrum of O_3 (from a dissociation threshold of $1.05 \text{ eV} = 1181 \text{ nm}$ to an ionization continuum of $30 \text{ eV} \approx 40 \text{ nm}$) was obtained in Ref. 21 by the method of the spectrum of electron losses at small angles for an energy of incident electron of 300 eV. It is depicted in Fig. 2. As is well known,^{25–26} the scattering cross section of high-energy electrons at small angles is proportional to the dipole moments of allowed dipole transitions and consequently, to the absorption cross section.

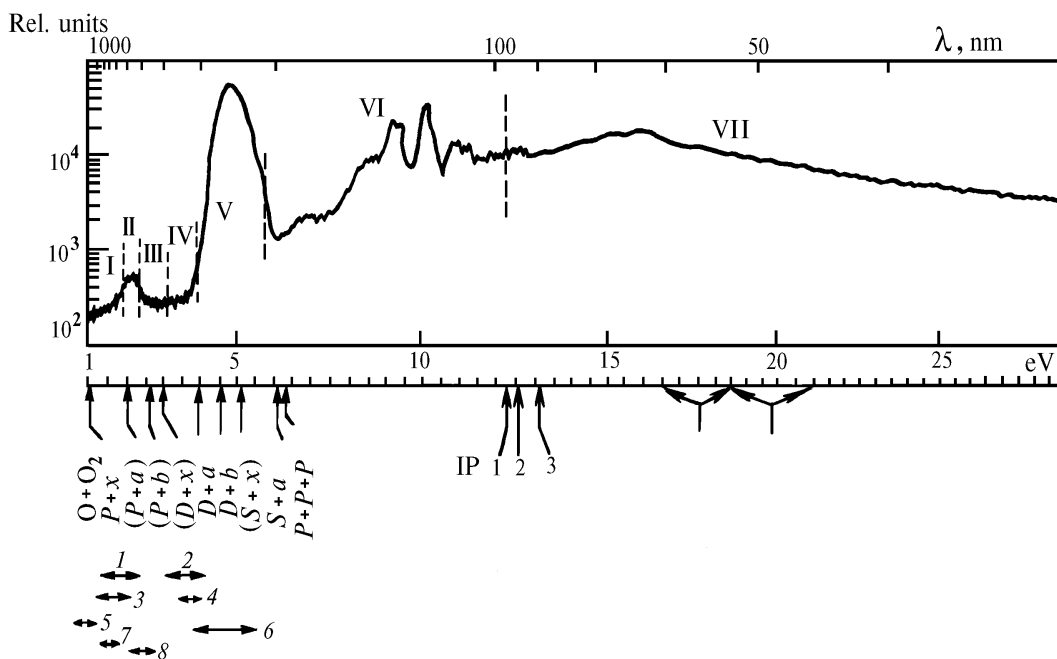


FIG. 2. Spectrum of electronic losses of O_3 measured in Ref. 21 with a resolution of 0.035 eV and the energy of incident electrons being equal to 300 eV. The vertical arrows indicate the dissociation thresholds, of O_3 (see Ref. 22) (forbidden spin combinations are given in parenthesis) and the ionization potentials (IP) (see Refs. 23 and 24). The following designations are used: $X \equiv O_2(X^3\Sigma_g^-)$, $a \equiv O_2(a^1\Delta_g)$, $b \equiv O_2(b^1\Sigma_g^+)$, $P \equiv O(^3P)$, $D \equiv O(^1D)$, and $S \equiv O(^1S)$. The horizontal arrows indicate the main absorption bands observed in infrared, visible, and ultraviolet regions: 1) Swanson–Celotta,^{68–69} 2) Huggins,⁴ 3) Wulf–Lefebvre,^{70–74} 4) Chalong–Lefebvre,⁷⁰ 5) Novick *et al.*,⁷⁷ 6) Hartley,² 7) Messmer–Salahub,⁷⁵ and 8) Chappuis³ bands.

From the near-infrared (1180 nm) to the far ultraviolet the ozone spectrum is diffusive due to dissociation or predissociation, and O_3 dissociates into O and O_2 with probability equal to unity. In Ref. 21 the spectrum was obtained with 0.035 eV resolution (~ 50 nm for the wavelength $\lambda \approx 1000$ nm, ~ 0.5 nm for $\lambda \approx 100$ nm, and ~ 0.05 nm for $\lambda \approx 50$ nm). Vertical lines and Roman numerals in Fig. 2 denote characteristic spectral regions described below in detail. For convenient interpretation of the spectrum shown in Fig. 2, the scheme of electronic states and transitions of the ozone molecule and products of its dissociation is shown in Fig. 3. The scheme summarizes the data of various approximate quantum-mechanical *ab initio* calculations and the experimental data as well. Only the levels up to 8 eV, corresponding to the single or double excitation of lower nonoccupied $2b_1 \pi^*$ -orbitals are shown in the figure.

Additional information is given in Tables I–III. Table I lists the dissociation energies of O_3 from the ground state X^1A_1 through different channels at a temperature of 0 K (see Refs. 7, 22, and 51). In the parenthesis the forbidden spin channels are indicated. The calculated values of equilibrium bond lengths and angles for the lower electronic states of O_3 are tabulated in Table II. The arrows indicate that in some states in C_{2v} symmetry the equilibrium states possess a lower C_s symmetry. Individual experimental data are marked in parenthesis. It was shown in Ref. 42 that the minima of states 1^1B_1 and 1^1A_2 also obey C_s symmetry; however, the quantitative calculations were made only in C_{2v} symmetry. In that very paper the second

local minimum of the state 1^1B_1 in C_{2v} symmetry was found (3.94 eV). It is marked by asterisk in Table II.

TABLE I.

| O_2 | Atomic oxygen | | | | | |
|-----------------|---------------|---|-------|--------|-------|---------|
| | 3P | | 1D | | 1S | |
| | nm | eV | nm | eV | nm | eV |
| $X^3\Sigma_g^-$ | 1180 | 1.05 ± 0.02 Refs. 52 and 53 1.066 ± 0.004 , Ref. 54 1.13, Ref. 55 | (410) | (3.01) | (324) | (5.24) |
| $a^1\Delta_g$ | (590) | (2.10) | 310 | 3.99 | 196 | 6.33 |
| $b^1\Sigma_g^+$ | (460) | (2.68) | 260 | 4.77 | 179 | 6.92 |
| $A^3\Sigma_u^+$ | 230 | 5.39 | (167) | (7.42) | (129) | (9.61) |
| $C^1\Sigma_u^-$ | (174) | (7.12) | – | – | – | – |
| $B^3\Sigma_u^-$ | 170 | 7.29 | (135) | (9.26) | (108) | (11.48) |
| $O(^3P)$ | 198 | 6.33 | – | – | – | – |
| $O(^3P)$ | | 6.315, Ref. 55 | – | – | – | – |

Table III lists the oscillator strengths and dipole moments of low-lying singlet states of O_3 . In the case of the state X^1A_1 , the magnitudes $(\partial\mu_x/\partial R)_0 = 0.75$ D/Å, $(\partial\mu_x/\partial\Theta)_0 = 0.74$ D/K, and $(\partial\mu_y/\partial R)_0 = 2.6$ D/Å were also determined theoretically and experimentally in Ref. 8. Here 1D (Debye) = 10^{-18} C.G.S.E.

TABLE II.

| State, ground configuration ⁸ | Symmetry | R(Å) | | θ (deg) | References, year |
|---|-----------------|--|----------------------|--|---|
| | | R ₁ | R ₂ | | |
| 1 | 2 | 3 | | 4 | 5 |
| 1 ¹ A ₁ (X ¹ A ₁) (normal ozone) ...4 b ₂ ² 6 a ₁ ² 1 a ₂ ² 1 b ₁ ² 79% 1 a ₂ ² → 1 b ₁ ² 11% | C _{2v} | 1.278 1.271 | | 116.8 116.8 | Ref. 56, 1956 (exp.) Ref. 57, 1970 (exp.) |
| 1 ¹ A ₁ (second minimum, ring ozone) 4 b ₂ ² → 2 b ₁ ² | D _{3h} | 1.48 1.449 1.422 1.435 1.426 1.434 1.48 1.46 1.44 1.45 1.470 | | 62 60 60 60 60 60 67 60 60 60 60 | Refs. 10 and 28, 1974 Ref. 22, 1977 Ref. 31, 1977 Refs. 33 and 45, 1977/78 Ref. 32, 1978 Ref. 14, 1980 Refs. 10 and 35, 1981 Ref. 36, 1984 Ref. 38, 1985 Ref. 10 and 39, 1985 Ref. 42, 1991 |
| 2 ¹ A ₁ 4 b ₂ ² → 2 b ₁ ² 36 % 6 b ₁ ² → 2 b ₁ ² 45 % | C _{2v} | 1.383 1.36 1.46 1.40 1.441 | | 90°36' 102.3 ≈135 86.5 116.8 (given) 83.592 | Ref. 90, 1966 (exp.) Ref. 45, 1978 (exp.) Ref. 35, 1981 Ref. 10, 1988 Ref. 41, 1990 Ref. 42, 1991 |
| Barrier between the two minima 1 ¹ A ₁ | C _{2v} | 1.418 1.41 ≈1.3 1.41 1.46 1.438; 1.431 | | 85 90 ≈80 85 86.5 83.574; 83.86 | Ref. 28, 1974 Ref. 34, 1979 Ref. 35, 1981 Refs. 36 and 37, 1984/85 Ref. 10, 1988 Refs. 42 and 58, 1990/91 |
| Crossing of 1 ¹ A ₁ and 2 ¹ A ₁ | C _{2v} | 1,4756 | | 83.1860 | Refs. 42 and 58, 1990/91 |
| Dissociation barrier 1 ¹ A ₁ | C _s | 1.234 | 1.759 | 114.90 | Ref. 42, 1991 |
| | C _{2v} | 2.007 | | 45 | Ref. 42, 1991 |
| 1 ³ B ₂ 1 a ₂ → 2 b ₁ ↓ 1 ³ A' | C _{2v} | 1.34 1.239 1.382 1.359 1.39 | | 108 114.9 107.9 109.6 110 | Ref. 27, 1974 Ref. 30, 1977 Ref. 22, 1977 Ref. 35, 1981 Refs. 36 and 37, 1984/85 |
| | C _s | 1.207 | 1.277 | 114,6 | Ref. 30, 1977 |
| 1 ¹ B ₁ 6 a ₁ → 2 b ₁ | C _{2v} | 1.34 1.370 1.354 1.482 1.785*) | | 117 117.7 116.8 (given) 117.50 46.27 | Ref. 27, 1977 Ref. 22, 1977 Ref. 41, 1990 Ref. 42, 1991 Ref. 42, 1991 |
| 1 ¹ B ₂ 1 a ₂ → 2 b ₁ ↓ 3 ¹ A' | C _{2v} | 1.50 1.405 1.453 1.482 | | 100 108.4 111.05 111.92 | Ref. 27, 1974 Ref. 22, 1977 Ref. 59, 1987 Ref. 42, 1991 |
| | C _s | 1.35 1.20 1.29 | 1.53 1.62 1.51 | — 108.4 70–106 116.8 (given) | Ref. 60, 1973 Ref. 22, 1977 Ref. 48, 1986 (exp.) Ref. 41, 1990 |
| 1 ³ B ₁ 6 a ₂ → 2 b ₁ | C _{2v} | 1.33 1.347 1.31 | | 118 123.8 131 | Ref. 27, 1974 Ref. 22, 1977 Refs. 36 and 37, 1984/85 |
| 1 ³ A ₂ 4 b ₂ → 2 b ₁ | C _{2v} | 1.34 | | 99 | Ref. 27, 1974 |
| 1 ¹ A ₂ 4 b ₂ → 2 b ₁ | C _{2v} | 1.34 1.379 | | 99 99.58 | Ref. 27, 1974 Ref. 42, 1991 |

TABLE III.

| State | Energy, eV | Oscillator strength f | | Dipole moment of the state μ , D | | Transition moment from X^1A_1 , D |
|----------|---|--|---|---|---|-------------------------------------|
| | experiment | theory | experiment | theory | experiment $ \mu $ | theory |
| X^1A_1 | 0.00 | — | — | −0.517 Ref. 22, −0.546 Ref. 12 | 0.580±0.030 Ref. 56; 0.532±0.020 Ref. 86 | — |
| 1^1A_2 | the Swanson–Celotte bands ⁶⁹ 1.67; 1.80; 1.92; the Chappuis band ⁶⁶ | 0.0 Ref. 22, 1.5·10 ^{−5} Ref. 8 | 3,2·10 ^{−5} Ref. 66 | −0.220 Ref. 22 | — | 0.0 Ref. 22, 0.014 Ref. 41 |
| 1^1B_1 | the Chappuis 2.0–2.3 band | 4.0·10 ^{−5} Ref. 22, 1.5·10 ^{−5} Ref. 8 | 2.0·10 ^{−5} Ref. 87; 3.2·10 ^{−5} Ref. 66 | −0.156 Ref. 22 | — | 0.0107 Ref. 22, 0.0182 Ref. 41 |
| 2^1A_1 | the Higgins 3.5–4.2 band (max 3.7) | 2.0·10 ^{−6} Ref. 22, 9.4·10 ^{−6} Ref. 8 | ~1·10 ^{−4} Ref. 45 | 0.221 Ref. 22 | — | 0.0107 Ref. 22, 0.0210 Ref. 41 |
| 1^1B_2 | the Hartley 4.1–5.7 band (max 4.86) | 0.230 Ref. 22, 0.176 Ref. 8 | 8.8·10 ^{−2} Ref. 87 | −0.126 Ref. 22 | — | 3.1222 Ref. 22, ~1.4 Ref. 41 |
| 2^1B_2 | — | 2·10 ^{−4} Ref. 8 | — | — | — | — |
| 2^1B_1 | Tanaka and Inn ⁸⁸ and Celotta et al. ²¹ with wide maximum ^{7,18} | 1.4·10 ^{−3} Ref. 8 | — | — | — | — |
| 3^1A_1 | — | 5·10 ^{−6} Ref. 8 | — | — | — | — |

One general comment should be made about the pressure dependence of the ozone spectrum. The pressure dependence of the electronic spectrum of O_3 was not observed because the Doppler broadening substantially exceeded the collisional (impact) one at temperatures and pressures of gases being investigated by now. The simple estimates confirm this fact.

The Doppler and collisional (impact) linewidths of atoms and molecules are given by formulas⁶¹

$$\Delta\lambda_D/\lambda = \frac{2}{c} \sqrt{\frac{2 \ln 2 R T}{m}} \lambda, \quad (1)$$

$$\Delta\lambda_{col}/\lambda = \frac{4 N_0}{c \sqrt{p m R T}} \sigma^2 p \lambda^2, \quad (2)$$

respectively, where λ is the wavelength, c is the speed of light, R is the universal gas constant, N_0 is the Avogadro number, m is the mass of an atom or molecule or the reduced mass of colliding particles, T is the temperature (in K), p is the pressure, and σ^2 is the squared effective radius of colliding particles. For $\lambda = 700$ – 1000 nm at $T = 200$ – 1000 K corresponding to the energy ranging from the dissociation threshold to the ionization energy and temperature interval for

which the ozone spectrum was examined, the substitution of the data on O_3 broadened by O_3 , O_2 , and N_2 (the value of σ^2 was taken from Ref. 62) gives the following relations:

$$\Delta\lambda_D/\lambda \approx (1.5\text{--}3.3) \cdot 10^{-6}, \quad (3)$$

$$\Delta\lambda_{col}/\lambda \approx (3.5\text{--}10) \cdot 10^{-9} p \text{ (Torr)}. \quad (4)$$

Estimate (4) from formula (2) agrees well with theoretical and experimental data on the impact broadening coefficients of pure rotational and rovibrational lines of O_3 broadened by O_3 , O_2 , and N_2 (see Refs. 63 and more recent Refs. 64 and 65).

It follows from estimates (3) and (4) that at $p \leq 1$ atm $\Delta\lambda_D > \Delta\lambda_{col}$. Because of predominant Doppler broadening of the electronic–rovibrational lines at $p \leq 1$ atm, appreciable overlapping of individual lines and diffuseness of the visible and UV spectra of O_3 , the impact line broadening in the case of electronic transitions of O_3 was not studied experimentally, as it was done for a number of IR rovibrational and pure rotational lines.^{64–65}

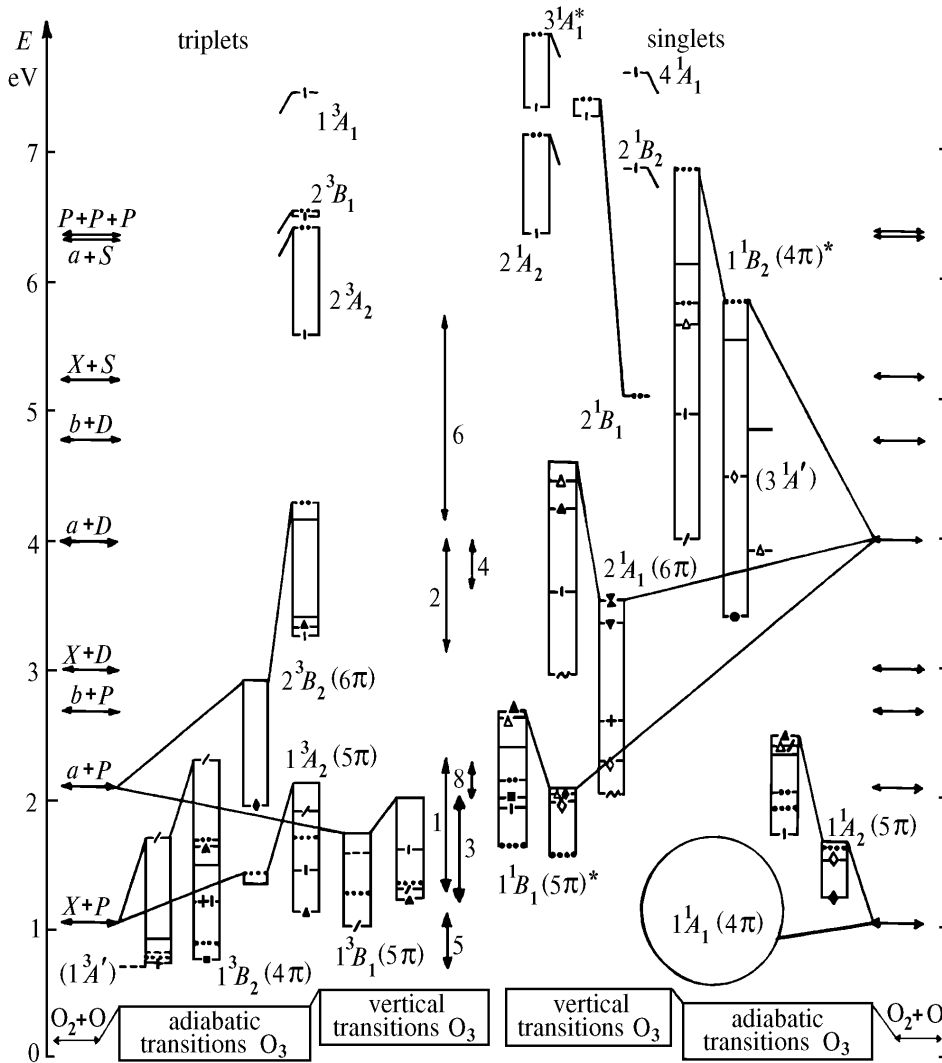


FIG. 3a. The scheme of electronic states of O_3 up to 8 eV for single- and two-electron excitations of the lower nonoccupied $2b_1 \pi^*$ -orbitals and products of dissociation. The horizontal lines denote the theoretical results (ab initio calculations): 1974, Ref. 27, -o- 1974, Ref. 28, -...- 1975, Ref. 7, --- 1977, Refs. 22 and 29, - - - 1977, Ref. 30, -x- 1977, Ref. 31, - · - 1978, Ref. 32 (models a and b), -| - 1978, Ref. 8, - \ - 1977/79, Refs. 33 and 34, - - 1980, Ref. 14, - + - 1981, Ref. 35, - / - 1984/85, Refs. 36 and 37, - v - 1985, Ref. 38, - ^ - 1985, Ref. 39, - ~ - 1988, Ref. 10, - \nabla - 1990, Ref. 40, - \Delta - 1990, Ref. 41, - \diamond - 1991, Ref. 42. The indirect experimental data: - \nabla - 1970, Ref. 43, - - 1974/75, Ref. 44, - X - 1978, Ref. 45, - \Delta - 1979, Ref. 46, - * - 1982, Ref. 47, - · - 1986, Ref. 48, and - \blacklozenge - 1990/91, Refs. 49 and 50. The double vertical and horizontal arrows indicate the experimental data on the absorption bands and dissociation thresholds of O_3 (see notation in Fig. 2). Adiabatic levels are joined with the levels of vertical transitions and with the levels of states of dissociation products being correlated with these surfaces. The data for the same surface are joined by vertical straight lines. The nomenclature of states is given in C_{2v} symmetry. The notation of states in the lower C_s symmetry is in parenthesis. Asterisks denote the states for which one-electron dipole transitions from the lower state X^1A_1 are allowed. The complex structure of the lower state 1^1A_1 in the general view of Fig. 3a is denoted conventionally by a circle and is shown separately on an enlarged scale in Fig. 3b.

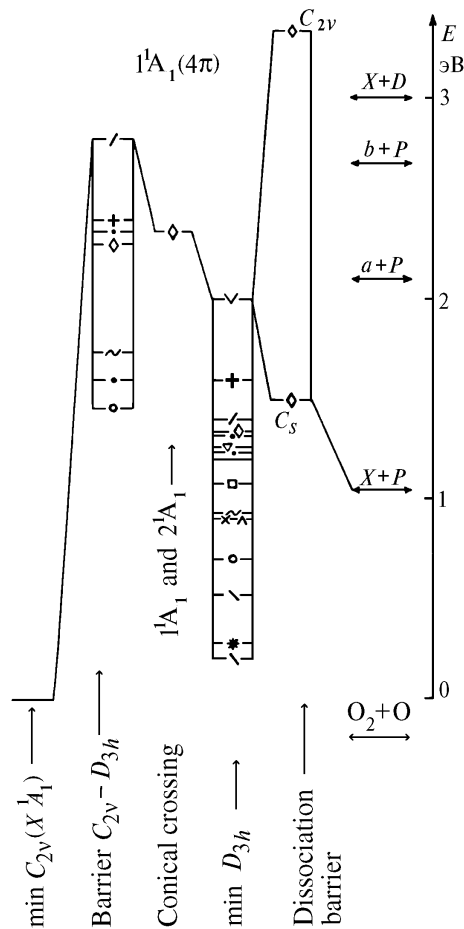


FIG. 3b.

It should be also noted that the data summarized in Ref. 63 pertain to the ozone spectra in the gas phase. However, the problem referred to as the *ozone hole problem* appeared to be closely related to the photochemical heterogeneous processes in clouds. This fact attracted particular interest to the heterogeneous catalytic cycles involving ozone, ozone cluster chemistry, and chemistry of condensed media. Of great interest is also the study of absorption and dissociation spectra of ozone under heterogeneous conditions in solutions and solid phase at lower temperatures. The papers of this kind were few in number and most of them were published 20–30 years ago (see Ref. 66 and references therein). However, in recent years the similar investigations have been resumed.^{66–67} They consider the transformation of the main (Chappuis, Huggins, and Hartley) absorption bands of O_3 in water and CCl_4 solutions at room temperature, in freon and O_2 solutions at $T = 77$ K, and in pure solid ozone (in thin films) and ozone put in ice as compared with the gas phase. The obtained data, namely, considerable increase of the absorption in the visible range as compared with the UV range, shifts of the band maxima whose magnitude and direction depend on temperature and solvent, spectral broadening, transformation of the spectrum, etc. are of considerable importance for further investigations of effect of heterogeneous processes on the ozone holes and yield additional information about the gas-phase spectra, although they are as yet qualitative in character. The main studies in this direction need to be done.

2. ENERGY REGION NEAR A LOWER DISSOCIATION THRESHOLD OF O_3 OF 1.05 EV (REGION I)

A few spectral observations of O_3 in the energy region near 1 eV, i.e., near the energy of the O_3 dissociation into unexcited O and O_2 products, where O_3 has no allowed dipole transitions, have been mentioned in the literature several times (see Fig. 3).

2.1 Measurements above the dissociation threshold

The Swanson–Celotta band. The papers by Swanson and Celotta^{68–69} should be mentioned above all. They observed a wide band of electrons with 4–8 eV energy scattered on ozone molecules at angles of $\sim 45^\circ$, $\sim 75^\circ$, and $\sim 90^\circ$ near an energy of about 1.65 eV (1.3–2.3 eV ≈ 950 –550 nm, yielding peaks of 1.29, 1.43, 1.55, 1.67, 1.80, and 1.92 eV). As is known,²⁶ contrary to the spectrum of high-energy electron losses at small scattering angles,²¹ the spectrum of low-energy (near-threshold) electron losses at large angles is primarily determined by forbidden electronic transitions, i.e., in the given case by exchange transitions from the low-lying singlet state X^1A_1 to one of the triplet states 3B_2 , 3B_1 , and 3A_2 or by electric quadrupole transition $X^1A_1 \rightarrow 1^1A_2$. According to the scheme shown in Fig. 2 and Table III, the transition $X^1A_1 \rightarrow 1^3B_2$ is expected to be most intense. In this case the state 1^3B_2 is probably weakly bound, because, according to some theoretical calculations,^{22,27,29,30,35,44} its adiabatic energy lies 0.1–0.3 eV lower than the dissociation threshold, especially when the stabilization of the state due to deformation of linear bonds of the molecule to lower C_s symmetry (and to the corresponding state $1^3A'$ in this symmetry) is taken into account.

The Wulf and Lefebvre bands. The other manifestations of the ozone electronic state near the dissociation threshold are the so-called Wulf 600–100 nm bands^{49,70–73} and the Lefebvre 650–1000 nm bands,⁷⁴ which are apparently pertinent to the electronic forbidden dipole transition and vibrational transition $X^1A_1 \rightarrow 1^1A_2$ allowed in the case of antisymmetric stretching.^{49,71} This transition may partially contribute to the above-mentioned Swanson–Celotta band as well as to the Chappuis band (see below). The 1.24 eV band found in Ref. 75 should be also mentioned.

Dye-laser excited UV transition spectrum of O_3 . McGrath and Thompson⁷⁶ studied the dye-laser excited UV transition spectrum of the ozone molecules at a wavelength of 320 nm. The authors ascribe this transient state to the electronic state 1^1A_2 and determined the radiative lifetime of the state 1^1A_1 $\tau = (4.10 \pm 0.95) \mu s$ as well as the rate of its decay in collisions with O_3 and He molecules $\kappa < 10^{-18} \text{ cm}^3/\text{s}$ from the analysis of the UV spectrum. Both values differ by several orders of magnitude from the previous estimates reported in the literature more than ten years ago (it was believed that $\tau \approx 1 \text{ s}$ [see Ref. 76] and $\kappa \sim 10^{-15} \text{ cm}^3/\text{s}$ [see Ref. 43]).

The IR spectrum^{16,18} of O_3 near 1 μm . Anderson et al.⁴⁹ analyzed in detail the absorption spectrum of two ozone isotopes in the region of the Wulf and Lefebvre bands. They assigned it to the dipole transition

$X^1A_1 \rightarrow 1^1A_2$ allowed for antisymmetric stretching. They also identified the vibrational structure of 1^1A_2 and determined its adiabatic energy under this assumption. The vibrational quanta of $^{16}O_3(1^1A_2)$ $\nu'_1 = 1200 \text{ cm}^{-1}$, $\nu'_2 \approx (528 \pm 15) \text{ cm}^{-1}$, and $\nu'_3 \approx (90 \pm 80) \text{ cm}^{-1}$ were obtained from this analysis.

2.2. Measurements below the dissociation threshold

Photoelectron detachment spectrum.

The $6000\text{--}9000 \text{ cm}^{-1}$ ($0.7\text{--}1.1 \text{ eV}$) band mentioned in Ref. 77 should be referred to the forbidden dipole transitions. It was observed in Ref. 77 but was not identified by the authors in their experiments on electron detachment from the negative ozone ions irradiated by the Ar- and dye-lasers.

One more corroboration of existence of electronic ozone states below the dissociation threshold comes from the data on photodissociation of positive⁴⁷ and negative⁷⁸ ozone ions obtained by Hiller and Vestal. These results in combination with the data on energy of O_3 and O and on the electron affinity for ozone and molecular oxygen yield highly underestimated threshold of O_3 dissociation into $O(^3P)$ and $O_2(^3\Sigma_g^-)$: $\leq 0.761 \pm 0.007 \text{ eV}$ (see Ref. 47) and $(0.747 \pm 0.013) \text{ eV}$ (see Ref. 78). It follows from references therein that this situation is peculiar to measurements of dissociation energy, i.e., the calorimetric methods give the values of the order of $1.02\text{--}1.05 \text{ eV}$ (see Ref. 79), whereas the spectroscopic methods give lesser values ($0.7\text{--}0.8 \text{ eV}$). One of the possible ways of resolving this contradiction is the assumption^{47,78} on the existence of a bound electronic state of O_3 below the dissociation threshold with an energy of $(0.28 \pm 0.01) \text{ eV}$.

The IR fluorescence near $1.9 \mu\text{m}$. In the study of UV-photolysis of O_3 Shi and Barker⁸⁰ observed IR-fluorescence in some bands in the wavelength region $2\text{--}10 \mu\text{m}$. Among these bands only the $1.9 \mu\text{m}$ band (centered at $(1.95 \pm 0.05) \mu\text{m}$ with a bandwidth of $\sim 0.15 \mu\text{m}$) was identified by the authors based on the circumstantial evidence as the transition between the electronic states of O_3 probably from a triplet state to one of its lower states. In the authors' opinion, the molecule transforms from the 1^1B_2 state (the upper electronic state in the Hartley band) into the presumed triplet state in collision with O_2 or Xe by singlet-triplet reaction of the type $O_3(1^1B_2) + O_2(^3\Sigma_g^-) \rightarrow O_3(^3\beta) + O_2(^1\Delta_g; ^1\Sigma_g^+)$ or $O_3(1^1B_2) + Xe \rightarrow O_3(^3\beta) + Xe$. There is no more detailed information about the state $^3\beta$ of O_3 and a character of radiation at $1.9 \mu\text{m}$ [$O_3(^3\beta) \rightarrow O_3(\gamma) + h\nu$] in Ref. 80, although the projected investigation of other observable fluorescent bands will probably elucidate these problems.

The ozone precursor. Beginning with Ref. 43, so-called precursor of O_3 was repeatedly discussed as an excited state of the ozone molecule whose energy is below the dissociation threshold. It was repeatedly observed in experiments involving processes of recombination (see, for example, Refs. 22 and 34 as well as 43-44) and was not unambiguously identified. Although the possibility of identification of the ozone precursor with the vibrationally-excited molecules was not ruled out in the most of papers referred to it, more often the authors followed the viewpoint that the bound states 1^3B_2 or/and the ring states

of O_3 (see below) form this excited state. In Ref. 44 the probability of formation of not only the vibrationally-excited ordinary ozone molecule but also the ozone molecules in bound electronic state (probably, 1^3B_2) by the recombination reaction ($O + O_2 + M \rightarrow O_3 + M^*$) was estimated together with the level of their vibrational excitation. This estimate was obtained from the analysis of luminescence of the state 1^3B_2 in the region near 800 nm ($\sim 1.55 \text{ eV}$). The authors of Ref. 35 believed that the ozone molecule could be found in the state 1^3B_2 no less frequently than in the state X^1A_1 .

The ring ozone. The probable candidate to the electronic ozone state with an energy of 0.28 eV (see Refs. 47 and 48) and to the above-mentioned precursor is, in addition to the state 1^3B_2 , the so-called ring (or cyclic) ozone, namely, the electronic ozone state of D_{3h} symmetry with equal bond lengths between the three O atoms and equal angles of 60° . The existence and the energy of the low-lying ring isomer of ordinary ozone have been long-standing problems for theoreticians and experimenters, since this isomer was calculated theoretically.²⁰ Various computations give the adiabatic energy of the ring ozone varying from the value being less (!) than its ground state energy⁸¹⁻⁸² to the value being 1.5 eV greater than the ground state energy, i.e., considerably exceeding the dissociation energy (see, for example, Refs. 22 and 31 and more recent Refs. 40 and 42, as well as Fig. 3). The vibrational frequencies of the ring ozone were determined, namely, doubly degenerated $\nu_2(e') = 750 \text{ cm}^{-1}$ (Ref. 42) and 795 cm^{-1} (Ref. 40) as well as $\nu_1(a'_1) = 1046 \text{ cm}^{-1}$ (Ref. 42) and 1114 cm^{-1} (Ref. 40).

The ring state of O_3 possesses D_{3h} symmetry, and in C_{2v} symmetry it forms the state 1^1A_1 . Although it has the same symmetry as the ground state X^1A_1 , the interaction between them is weak, because the transition $X^1A_1 \rightarrow 1^1A_1$ is the two-electron and, correspondingly, forbidden dipole transition. However, since the minimum of energy of the ring ozone is near the dissociation threshold and the diabatic excited state 1^1A_1 correlates with excited dissociation products of O_3 [$O(^1D) + O_2(^1\Delta_g)$], in this case the surfaces X^1A_1 and 1^1A_1 cross and/or repulse. Even the weak interaction of surfaces in this region might play an important role in the formation of electronic structure and ozone spectra.

From theoretical analysis based on *ab initio* calculations with the exception of Refs. 42 and 58 (see Fig. 3 and Table II) the following pattern of interaction between the electronic surfaces X^1A_1 and 1^1A_1 is outlined. The lower energy level of the state 1^1A_1 lies between the minimum energy level of the ground state X^1A_1 and a dissociation threshold of 1.05 eV or, probably, slightly higher. As the value of the vertex angle and the lengths of the side bonds of the molecule change (see Fig. 1a), the diabatic potential surfaces X^1A_1 and 1^1A_1 cross and the lower adiabatic surface 1^1A_1 is formed as a result of repulsion in the region of crossing. It has two energy minima^{10,34} - the principal minimum X^1A_1 ($\vartheta = 116.8^\circ$ and $R_1 = R_2 = 1.27 \text{ \AA}$) and the ring minimum ($\vartheta = 60^\circ$ and $R = 1.43\text{--}1.48 \text{ \AA}$) which is named the second energy minimum of the state 1^1A_1 in

Table II. Between these minima there is a potential energy barrier^{10,28,32,34–37,42} lying near or somewhat higher than the energy of dissociation $O(^3P) + O_2(^3\Sigma_g^-)$ (region of avoided crossing of diabatic surfaces X^1A_1 and 1A_1). The angle and the bond lengths of the molecule in the region of potential energy barrier are intermediate between the angles and bond lengths corresponding to energy minima ($\theta \approx 84\text{--}90^\circ$ and $R_{1,2} \approx 1.4 \text{ \AA}$). The above-described pattern is shown in Fig. 1a. According to the data of Refs. 8–10, near the principal energy minimum the contribution of the ground configuration $\dots 4b_2^2 6a_1^2 1b_1^2 1a_2^2$ to this surface is about 79%, while the contribution of configuration corresponding to the two-electron transition $1a_2^2 \rightarrow 2b_1^2$ is about 11%, as described in Sec. 1. In the region of cyclic isomer this surface consists of the configuration $\dots 4b_2^0 6a_1^2 1b_1^2 1a_2^2 2b_1^2$ (two-electron transition from the ground configuration $4b_2^2 \rightarrow 2b_1^2$). The lower surface might have one more energy barrier for dissociation,^{30,42,83} however, its value predicted in Ref. 30 and newly discovered in Ref. 42 (see Figs. 1 and 3) is, probably, highly overestimated (according to the analysis of Ref. 16, it is no more than 0.04 eV). The upper adiabatic surface 2^1A_1 is correlated with the excited dissociation products and has more complex structure than that shown in Fig. 1a because of crossing with higher potential surfaces (see Fig. 1b). According to Ref. 8, in the region of the principal minimum of the state X^1A_1 the contribution of the cyclic configuration to this surface is 36% and that of the configuration $\dots 4b_2^2 6a_1^0 1b_1^2 1a_2^2 2b_1^2$ is 45% (two-electron transition from the ground configuration $6a_1^2 \rightarrow 2b_1^2$). This surface is responsible for absorption in the Huggins bands and is considered below in detail.

There are, however, the data on the structure of potential surfaces in 1A_1 symmetry which differ slightly from the above-described scheme, although they do not radically contradict it. In the preliminary report⁵⁸ and then in the detailed paper⁴² Xantheas et al. presented the results of *ab initio* calculations by the method of multiconfiguration self-consistent field in the complete valence space in the entire region of transition between cyclic and open structures of the ozone molecule. They pioneered that near the barrier open ozone — ring ozone the conical crossing was observed of the potential surfaces of the same symmetry (1A_1 in C_{2v} symmetry and $^1A'$ in C_s symmetry), namely, the adiabatic surface of the ground state 1A_1 (with two local minima, open and ring) and of the state 2^1A_1 . In Ref. 42 it was demonstrated that this crossing, in complete accordance with conics, is of a point character in C_{2v} symmetry ($\theta = 83.1860^\circ$ and $R = 1.4756 \text{ \AA}$), near the top of the potential barrier ($\theta = 83.574^\circ$ and $R = 1.438 \text{ \AA}$, see Table II) is spaced only at 0.038 Å from it, and in unequal-sided geometry of C_s symmetry goes over to a one-dimensional line of crossing being nearly parallel to the ridge of the potential barrier with the energy gap between them of about $\approx 1.2 \cdot 10^{-3} \text{ amu} = 0.03 \text{ eV}$. In addition, the authors of Ref. 42 found that the minimum of the upper crossing surface 2^1A_1 is also very close to the barrier and to the point of conical crossing ($\theta = 83.592^\circ$ and $R = 1.441 \text{ \AA}$) being 0.004 eV above the barrier and 0.026 eV below the

point of crossing. In other words, the transition between two minima 1A_1 , the minimum 2^1A_1 , and the point of conical crossing of 1A_1 and 2^1A_1 are all within 0.04 Å and are spaced at 0.04 eV. It was also proved that the barrier between the minima 1A_1 and the minimum 2^1A_1 is strictly realized in C_{2v} symmetry whereas the second minimum 1A_1 (ring ozone) is appeared in D_{3h} symmetry. Consequently, the complete transition from the ring ozone to the open ozone takes place in C_{2v} symmetry. Since the bond lengths corresponding to the barrier and ring ozone are close in values, this transition is practically pure bending motion.

This structure of surfaces (not shown in Fig. 1a) undoubtedly complicates the above-described pattern but does not contradict it. If the results of calculations performed in Refs. 42 and 58 are corroborated, it will be one of a great number of evidences for the existence of conical crossing in nature, the question of which has long been discussed in the literature with a large portion of scepticism (see the review of related papers in Ref. 42). In C_{2v} symmetry for the ground molecular state the conical crossing was obtained for the first time.

In addition to calculations of the minima 1A_1 and 2^1A_1 and their transient states, the authors of Ref. 42 analyzed the dissociation of the states 1A_1 , although to a less accuracy. According to the results of their computations, the dissociation of the ozone molecule in C_{2v} symmetry (detachment of a central atom) is extremely unfavorable, namely, the barrier to this process from the state X^1A_1 is more than 3.3 eV. The most favorable channel of dissociation is the detachment of the external oxygen atom in C_s symmetry. There is also a barrier to this process with a saddle of about 0.5 eV above the threshold of dissociation into $O + O_2$. The angle at this point is close to the angle of the ground state X^1A_1 , i.e., the ozone molecule dissociates nearly without bending motion.

It is possible that the data of Refs. 42 and 58 point to the improper representation of the state 1A_1 as a one-sheeted potential surface, which is in contradiction with the opinion of most explorers. According to the results of recent calculations,⁸⁴ one-sheeted surface 1A_1 yielding unexcited products of dissociation is a good model for calculations of many characteristics of O_3 . Varandas and Pais⁸⁴ proposed a new semiempirical model of this surface with the parameters adjusted to the results of *ab initio* calculations and experimental data on a number of characteristics of O_3 .

The alternative model¹⁶ of two-sheeted surface with two diabatic surfaces, one of them being mentioned above and another describing the excited dissociation products $O(^1D) + O_2(^1\Delta_g)$, may be also used. The model, reported in Ref. 16 and developed by the authors of Ref. 84, was criticized in Ref. 84 although none of the proposed models was adequate in all respects. As for applications, the one-sheeted model is obviously more convenient. In addition, the model proposed in Ref. 84 not only adequately describes the equilibrium region of states as compared with the results of *ab initio* calculations, but gives the real asymptotic as well, that places it presumably among the best one-sheeted approximations of the surface 1A_1 .

2.3. Conclusions

Let us enumerate the above-discussed properties of the electronic states of the ozone molecule near dissociation energy of 1.05 eV. Experimentally observed in this region are the following bands:

- 1.3–2.3 eV (reaching maximum of about 1.6–1.7 eV) forbidden transition band in the scattering spectrum of the near-threshold energy at large angles,⁶⁸
- Wulf 1.2–2 eV vibrational bands,^{49,70–73,85}
- Lefebvre 1.2–1.9 eV vibrational band,^{74,85}
- Anderson et al.^{16,18} vibrational bands near 1 μm in the absorption spectrum of O₃ isotops,⁴⁹
- 0.7–1.1 eV band in the spectrum of photodetachment of an electron from the negative ozone ion O₃⁻ (see Ref. 77),
- weak absorption near 1.24 eV (see Ref. 75),
- nonidentified electronic state with an energy of (0.28 \pm 0.01) eV as an alternative to the inconsistency in measurements of the dissociation energy by calorimetric and spectroscopic methods (in particular, by the methods of photodissociation of positive⁴⁷ and negative⁷⁸ ozone ions),
- formation of some nonidentified ozone states near 1 eV (the ozone precursor) by different photochemical and ionic reactions, mainly, recombination reactions,^{22,34,43–44} and
- UV transition spectrum of O₃ (320 nm) excited by a dye-laser.⁷⁶

It was shown theoretically that in the above-considered energetic region the ozone molecule has three triplet states 1^3B_2 , 1^3A_2 , and 1^3B_1 , of which the state 1^3B_2 may be weakly bound relative to the dissociation into unexcited products. Additionally, in this region there is the dissociative state 1^1A_2 with a radiative lifetime of (4.10 \pm 0.95) μs (see Ref. 76) (the transition $X^1A_1 \rightarrow 1^1A_2$ is the electric quadrupole transition, and is vibrationally allowed for antisymmetric stretching in dipole approximation) and, probably, the bound or weakly bound state 1^1A_1 (the second minimum), representing the ring structure of ozone and forming with the lower state X^1A_1 the adiabatic potential surface with two minima (both lying below the dissociation energy) and the intermediate barrier of the order of or above the dissociation energy (the transition $X^1A_1 \rightarrow$ the second minimum of the state 1^1A_1 is the two-electron transition). However, it is possible, that the interaction of the surfaces 1^1A_1 and 2^1A_1 (their conical crossing) does not allow one to consider the surface X^1A_1 in all cases as a one-sheeted surface,^{16,58} although the one-sheeted surface is a very adequate model⁸⁴ for many applications and can be used for calculation of various ozone characteristics.

The locations of calculated surfaces agree with the experimentally observed transitions; however, there are no experiments so far, which could unambiguously determine the energy and identify the above-described electronic states. Of particular interest is here the evidence of existence of metastable ring ozone (for example, in luminescence on the transition to the ground state), since because of the predicted location of the ring ozone it might play an important role in the atmospheric photochemical processes and in the laboratory IR photochemistry of ozone.

REFERENCES

1. Ch.F. Schönbein, L. de M. Schönbein, and M. Arago, *Comptes Rendus* **10**, No. 17, 706 (1840).
2. W.N. Hartley, *J. Chem. Phys.* **39**, 57 (1881).
3. J. Chappuis, *Comptes Rendus* **94**, No. 15, 858 (1882).
4. W. Huggins and Mrs. Huggins, *Proc. Roy. Soc. A* **48**, 216 (1890).
5. D.R. Salahub, S.H. Lamson, and R.P. Messmer, *Chem. Phys. Lett.* **85**, No. 4, 430 (1982).
6. V.R. Saunders and J.H. von Lenthe, *Mol. Phys.* **48**, No. 5, 923 (1983).
7. P. J. Hay, T.H. Dunning, Jr., and W.A. Goddard III, *J. Chem. Phys.* **62**, No. 10, 3912 (1975).
8. K.-H. Thunemann, S.D. Peyerimhoff, and R.J. Buenker, *J. Mol. Spectrosc.* **70**, No. 3, 432 (1978).
9. W.D. Laidig and H.F. Schaefer III, *J. Chem. Phys.* **74**, No. 6, 3411 (1981).
10. F. Moscardo, R. Andarias, and E. San-Fabian, *Int. J. Quant. Chem.* **34**, No. 4, 375 (1988).
11. R.D. Harcourt, F.L. Skrzewek, R.M. Wilson, and R.H. Flegg, *J. Chem. Soc. Farad. Trans. II* **82**, No. 4, 495 (1986).
12. K.A. Peterson, R.C. Mayrhofer, E.L. Sibert III, and R.C. Woods, *J. Chem. Phys.* **94**, No. 1, 414 (1991).
13. K.V. Ermakov, B.S. Butaev, and V.P. Spiridonov, *J. Mol. Struct.* **240**, 295 (1990).
14. J.S. Wright, S.-K. Shin, and R.J. Buenker, *Chem. Phys. Lett.* **75**, No. 3, 513 (1980).
15. M.G. Sheppard and R.B. Walker, *J. Chem. Phys.* **78**, No. 12, 7191 (1983).
16. S. Carters, I.M. Mills, J.N. Murrell, and A. J. C. Varandas, *Mol. Phys.* **45**, No. 5, 1053 (1982).
17. J.M. Standard and M.E. Kellman, *J. Chem. Phys.* **94**, No. 7, 4714 (1991).
18. A.D. Walsh, *J. Chem. Soc.* **3**, No. 8, 2266 (1953).
19. R.S. Mulliken, *Can. J. Chem.* **36**, No. 1, 10 (1958).
20. S.D. Peyerimhoff and R. J. Buenker, *J. Chem. Phys.* **47**, No. 6, 1953 (1967).
21. R. J. Celotta, S.R. Mielczarek, and C.E. Kuyatt, *Chem. Phys. Lett.* **24**, No. 3, 428 (1974).
22. P. J. Hay and T.H. Dunning, Jr., *J. Chem. Phys.* **67**, No. 5, 2290 (1977).
23. C.R. Brundle, *Chem. Phys. Lett.* **26**, No. 1, 25 (1974).
24. D.S. Frost, S.T. Lee, and C.A. McDowell, *Chem. Phys. Lett.* **24**, No. 2, 149 (1974).
25. S. Trajmar, J.K. Rice, and A. Kuppermann, *Adv. Chem. Phys.* **18**, 15 (1970).
26. M. Inokuti, *Rev. Mod. Phys.* **43**, No. 3, 297 (1971).
27. D.V. Grimbert and A. Devaquet, *Mol. Phys.* **27**, No. 4, 831 (1974).
28. S. Shin, R. J. Buenker, and S.D. Peyerimhoff, *Chem. Phys. Lett.* **28**, No. 4, 463 (1974).
29. L.B. Harding and W.A. Goddard III, *J. Chem. Phys.* **67**, No. 5, 2377 (1977).
30. M. J. S. Dewar, S. Olivella, and H.S. Rzepa, *Chem. Phys. Lett.* **47**, No. 1, 80 (1977).
31. R.R. Lucchese and H.F. Schaefer, *J. Chem. Phys.* **67**, No. 2, 848 (1977).
32. G. Karlström, S. Engström, and B. Jönsson, *Chem. Phys. Lett.* **57**, No. 3, 390 (1978).
33. P.G. Burton, *Int. J. Quant. Chem.* No. 11, 207 (1977).
34. P.G. Burton, *J. Chem. Phys.* **71**, No. 2, 961 (1979).
35. C.W. Wilson, Jr. and D.G. Hopper, *J. Chem. Phys.* **74**, No. 1, 595 (1981).
36. R.O. Jones, *Phys. Rev. Lett.* **52**, No. 22, 2002 (1984).
37. R.O. Jones, *J. Chem. Phys.* **82**, No. 1, 325 (1985).

38. M. Morin, A.E. Foti, and D.R. Salahub, *Can. J. Chem.* **63**, No. 7, 1982 (1985).
39. W.G. Laidlaw and M. Trisic, *Can. J. Chem.* **63**, No. 7, 2044 (1985).
40. T. J. Lee, *Chem. Phys. Lett.* **169**, No. 6, 529 (1990).
41. A. Banichevich, S.D. Peyerimhoff, and F. Green, *Chem. Phys. Lett.* **173**, No. 1, 1 (1990).
42. S.S. Xantheas, G. J. Atchity, S.T. Elbert, and K. Ruedenberg, *J. Chem. Phys.* **94**, No. 12, 8054 (1991).
43. J.F. Riley and R.W. Cahill, *J. Chem. Phys.* **52**, 3297 (1970).
44. C.W. von Rosenberg, Jr. and D.W. Trainor, *J. Chem. Phys.* **61**, No. 6, 2442 (1974); **63**, No. 12, 5348 (1975).
45. J.C.D. Brand, K. J. Cross, and A.R. Hoy, *Can. J. Phys.* **56**, 327 (1978).
46. D.H. Katayama, *J. Chem. Phys.* **71**, No. 2, 815 (1979).
47. J.F. Hiller and M.L. Vestal, *J. Chem. Phys.* **77**, No. 3, 1248 (1982).
48. A. Sinha, D. Imre, J.H. Goble, Jr., and J.L. Kinsey, *J. Chem. Phys.* **84**, No. 11, 6108 (1986).
49. S.M. Anderson, J. Morton, and K. Mauersberger, *J. Chem. Phys.* **93**, No. 6, 3826 (1990).
50. S.M. Anderson, J. Maeder, and K. Mauersberger, *J. Chem. Phys.* **94**, No. 10, 6351 (1991).
51. A.A. Turnipseed, G.L. Vaghjiani, T. Gierczak, et al., *J. Chem. Phys.* **95**, No. 5, 3244 (1991).
52. D.R. Stull, H. Prophet, et al., NSRDS-NBS 37, Office of Standard Reference Data, National Bureau of Standards, Washington, DC, Contract No. FO4611-67-C-0009 (1971).
53. J.L. Gole and R.N. Zare, *J. Chem. Phys.* **57**, 5331 (1972).
54. M. J. Weiss, J. Berkowitz, and E.H. Appelman, *J. Chem. Phys.* **66**, No. 5, 2049 (1977).
55. R. Krishna and K.D. Jordan, *Chem. Phys.* **115**, No. 3, 423 (1987).
56. R.H. Hugnes, *J. Chem. Phys.* **24**, No. 1, 131 (1956).
57. T. Tanaka and Y. Morino, *J. Mol. Spectrosc.* **33**, No. 3, 538 (1970).
58. S.S. Xantheas, S.T. Elbert, and K. Ruedenberg, *J. Chem. Phys.* **93**, No. 10, 7519 (1990).
59. L.L. Lohr and A.J. Helman, *J. Chem. Phys.* **86**, No. 10, 5329 (1987).
60. A. Devaquet and J. Ryan, *Chem. Phys. Lett.* **22**, No. 2, 269 (1973).
61. S.É. Frish, *Optical Spectra of Atoms* (Fizmatgiz, Moscow, 1963), Ch. VII.
62. M.J. Kurylo, W. Braun, and A. Kaldor, *Chem. Phys. Lett.* **27**, 249 (1974).
63. J.I. Steinfeld, S.M. Adler-Golden, and J.W. Gallagher, *J. Phys. Chem. Ref. Data* **16**, No. 4, 911 (1987).
64. C. Flannery, J. J. Klassen, M. Gojer, et al., *J. Quant. Spectrosc. Radiat. Transfer* **46**, No. 2, 73 (1991).
65. M.N. Spencer and C. Chackerian, Jr., *J. Mol. Spectrosc.* **146**, No. 1, 135 (1991).
66. V. Vaida, D. J. Donaldson, S. J. Strickler, et al., *J. Phys. Chem.* **93**, No. 2, 506 (1989).
67. A. J. Sedlacek and C.A. Wight, *J. Phys. Chem.* **93**, No. 2, 509 (1989).
68. N. Swanson and R. J. Celotta, *Phys. Rev. Lett.* **35**, No. 12, 783 (1975).
69. R. J. Celotta, N. Swanson and M. Kurepa, in: *Abstracts of Reports at the 10th IPEAC Conference* (1977).
70. O.P. Wulf, *Proc. Natl. Acad. Sci. USA* **16**, No. 7, 507 (1930).
71. P. J. Hay and W.A. Goddard III, *Chem. Phys. Lett.* **14**, No. 1, 46 (1972).
72. P. J. Hay, T.N. Dunning, Jr., and W.A. Goddard III, *Chem. Phys. Lett.* **23**, No. 4, 457 (1973).
73. G. Herzberg, *Molecular Spectra and Molecular Structure. Vol. I. Spectra of Diatomic Molecules* (Van Nostrand, New York, 1939).
74. L.Lefebvre, *C.R Acad. Sci. (Paris)* **200**, No. 21, 1743 (1935).
75. R.P. Messner and D.R. Salahub, *J. Chem. Phys.* **65**, No. 2, 779 (1976).
76. W.D. McGrath, A. Thomson, and J. Trocha-Grimshaw, *Planetary Space Sci.* **34**, No. 11, 1147.
77. S.E. Novick, P.C. Engelking, P.L. Jones et al., *J. Chem. Phys.* **70**, No. 6, 2652 (1979).
78. J.F. Hiller and M.L. Vestal, *J. Chem. Phys.* **74**, No. 1, 6096 (1981).
79. S. Kuis, R. Simonaitis, and J. Heicklen, *J. Geophys. Res.* **80**, 28 (1975).
80. J. Shi and J.R. Barker, *J. Phys. Chem.* **94**, No. 22, 8390 (1990).
81. J.S. Wright, *Can. J. Chem.* **51**, No. 1, 139 (1973).
82. W.G. Laidlaw and M. Trisic, *Chem. Phys.* **36**, 323 (1979).
83. P. J. Hay, R.T. Pack, R.B. Walker, and E. J. Heller, *J. Phys. Chem.* **86**, No. 6, 862 (1982).
84. A. J. C. Varandas and A.A.C.C. Pais, *Mol. Phys.* **65**, No. 4, 846 (1988).
85. M. Griggs, *J. Chem. Phys.* **49**, No. 2, 857 (1968).
86. M. Lichtenstein, J. J. Gallagher, and S.A. Clough, *J. Mol. Spectrosc.* **40**, 10 (1971).
87. E.C.Y. Inn and Y. Tanaka, *J. Opt. Soc. Am.* **43**, No. 10, 870 (1953).
88. Y. Tanaka, E.C.Y. Inn, and K. Watanabe, *J. Chem. Phys.* **21**, No. 10, 1651 (1953).
89. L.A. Curtiss, S.R. Landghoff, and G.D. Cartney, *J. Chem. Phys.* **71**, No. 12, 5016 (1979).
90. C.-W. Lui and B.T. Darling, *J. Mol. Spectrosc.* **21**, No. 2, 146 (1966).